Nanoscale Res Lett (2009) 4:391–399
DOI 10.1007/s11671-009-9258-1

NANO EXPRESS

Synthesis and Characterization of Aromatic–Aliphatic Polyamide Nanocomposite Films Incorporating a Thermally Stable Organoclay

Sonia Zulfiqar · Muhammad Ilyas Sarwar

Received: 24 November 2008 / Accepted: 8 January 2009 / Published online: 30 January 2009

Abstract Nanocomposites were synthesized from reactive thermally stable montmorillonite and aromatic–aliphatic polyamide obtained from 4-aminophenyl sulfone and sebacoyl chloride. Carbonyl chloride terminal chain ends were generated using 1% extra sebacoyl chloride that could interact chemically with the organoclay. The distribution of clay in the nanocomposites was investigated by XRD, SEM, and TEM. Mechanical and thermal properties of these materials were monitored using tensile testing, TGA, and DSC. The results revealed delaminated and intercalated nanostructures leading to improved tensile strength and modulus up to 6 wt% addition of organoclay. The elongation at break and toughness of the nanocomposites decreased with increasing clay contents. The nanocomposites were thermally stable in the range 400–450 °C. The glass transition temperature increased relative to the neat polyamide due to the interfacial interactions between the two phases. Water uptake of the hybrids decreased upon the addition of organoclay depicting reduced permeability.

Keywords Nanocomposites · Polyamides · Nanostructure · Organoclay · Mechanical properties · Thermal properties

Introduction

There have been numerous reports describing the preparation and characterization of polymer-based clay nanocomposites. Typically, this involves reinforcing a polymer with modified clay (ceramic type filler). The degree of homogeneity and adhesion between the organic (polymer) and inorganic (clay) components can be improved using reactive organoclay, which results in greatly improved properties of the hybrid materials. The enhanced properties for these nanocomposites include mechanical [1–7], thermal [1–4], barrier [8, 9], flammability [4, 10–12] and are related to the dispersion and nanostructure of the layered silicate in the polymer matrix. The greater advantages come from the delaminated samples with the exception of flammability, where both delaminated and intercalated nanocomposites behave in the same way [10, 11]. Three preparative approaches are generally applied to obtain these hybrid materials: in situ polymerization intercalation, solution intercalation, and melt intercalation. Shen et.al. [13] have compared the solution and melt intercalation of polymer clay composites. Solution intercalation is a solvent-based technique in which polymer is soluble and clay is swellable. When they are both mixed, the polymer chains intercalate and displace the solvent within the interlayer of the silicate. Upon solvent removal, the intercalated structure remains, resulting in hybrids with nanoscale morphology. Morgan and Gilman [14] described factors affecting the nanostructure of composites, especially in melt intercalation. The most important point that they emphasized is the organic treatment, without which the dispersion of hydrophilic clay into hydrophobic polymer is impossible. Secondly, the importance of thermal stability of the organic modifier was also pointed out by the same group, particularly in melt blending or curing the nanocomposites at high temperature. The commonly employed alkyl ammonium ion as modifier for layered silicates is thermally unstable, degrading at temperatures of 200 °C or less. When this degradation

S. Zulfiqar · M. I. Sarwar (✉)
Department of Chemistry, Quaid-i-Azam University, Islamabad 45320, Pakistan
e-mail: ilyassarwar@hotmail.com

takes place, the silicate layers lose their organophilicity becoming hydrophilic again, and their ability to positively affect the physical properties may be reduced. The advantages expected from the nanocomposites usually deteriorate under these conditions. To overcome this difficulty, we have prepared an amine terminated aromatic amide oligomer (modifier), which is thermally stable and can also produce the interactions among the two phases. These nanocomposites find their applications in aerospace, automobile, and packaging industries.

Polyamides, the most versatile class of engineering polymers, display a wide range of properties. Aliphatic polyamides (nylons) find many industrial and textile applications due to their high mechanical strength and durability. Many studies on nylon-based clay nanocomposites have been reported previously [15–20]. Aromatic polyamides (aramids) are being used in industry because of their outstanding properties. However, poor solubility in common organic solvents and high melting temperatures are the limiting factors for the processing of these materials. A lot of attempts have been made to solubilize these polymers in order to prepare their composites using different techniques [21–25]. Aliphatic–aromatic polyamides (glass clear nylons) offer a wide range of properties including transparency, thermal stability, good barrier, and solvent resistant properties. These commercial polyamides have been reinforced with various ceramic phases [26–29]. There are numerous references to polyamides from aliphatic diamines and aromatic diacids and a far lesser number to polyamides from aromatic diamines and aliphatic diacids [30–38]. Probably the reason that aliphatic–aromatic polyamides have been studied in greater detail than the aromatic–aliphatic is that many of the former group can be made by melt and plasticized melt methods [32, 33, 39] or by standard interfacial procedures [35, 37, 40]. The aromatic–aliphatic polyamides, on the other hand are difficult to prepare by interfacial and solution methods [30, 41] and when prepared by melt methods, frequently are discolored and may have branched or network structures. Recently, excellent nanocomposites obtained from pectin–ZnO and ethylene vinylacetate–carbon nanofiber have been reported [42, 43]. Metal nanoparticle embedded conducting polymer–polyoxometalate composites and ionic liquid assisted polyaniline–gold nanocomposites for biocatalytic application have also been investigated [44, 45].

Keeping in view the importance of these polyamides, we have prepared the aromatic–aliphatic polyamide containing sulfone linkages by low temperature polycondensation method that could offer a balance of properties between those of tractable aliphatic nylons and the virtually insoluble and non-melting wholly aromatic polyamides. This aromatic–aliphatic polyamide is soluble in DMF, DMSO, and DMAc which can be attributed to the flexible sulfone linkages that provide a polymer chain with a lower energy of internal rotation [46]. This polyamide was reinforced with reactive, thermally stable montmorillonite intercalated with oligomeric species. The nanocomposites obtained by solution intercalation technique were characterized for XRD, SEM, TEM, mechanical testing, TGA, DSC, and water uptake measurements.

Experimental

Materials

The monomers, 4-aminophenyl sulfone (APS) 97%, sebacoyl chloride (SCC) 97%, 4-4′-oxydianiline (ODA) ≥98%, isophthaloyl chloride (IPC) ≥98% purchased from Aldrich were used as received. Triethylamine (TEA) ≥99.5%, dimethylsulfoxide (DMSO) ≥99.9%, methanol (99.8%), and hydrochloric acid >99% procured from Fluka were used as such. Montmorillonite K-10 (cation exchange capacity of 119 meq/100 g), silver nitrate (99.9%), and *N*, *N*-dimethyl acetamide (DMAc) >99% (dried over molecular sieves before use) obtained from Aldrich were used.

Synthesis of Amine Terminated Aromatic Amide Oligomer

Amide oligomer was synthesized by reacting ODA (2 mol) and IPC (1 mol) in DMAc under anhydrous conditions. Both the monomers were dissolved in DMAc separately and then mixed by drop wise addition of ODA into IPC solution with constant stirring. The reaction mixture was placed in the ice bath to avoid any side reactions. A stoichiometric amount of TEA was added to the contents of the flask with high speed stirring for 3 h in order to quench HCl produced during the reaction. Oligomerization reaction is shown in Scheme 1. The oligomer solution was precipitated in excess methanol, filtered, and then dried under vacuum.

Preparation of Oligomer-MMT

For the synthesis of nanocomposites, nature of the clay was first changed from hydrophilic to organophilic through an ion exchange reaction using oligomeric species as a modifier. Since oligomer was soluble in DMSO, the intercalation was carried out in the non-aqueous medium (Scheme 1). Solid oligomer (25.23 g) was dissolved in DMSO (100 mL) followed by slow addition of concentrated hydrochloric acid (4.8 mL) with constant stirring and heating at 80 °C. Montmorillonite was dispersed in another beaker in DMSO at 80 °C. This suspended clay was added to the cationic oligomer solution with stirring at 60 °C for 3 h. The

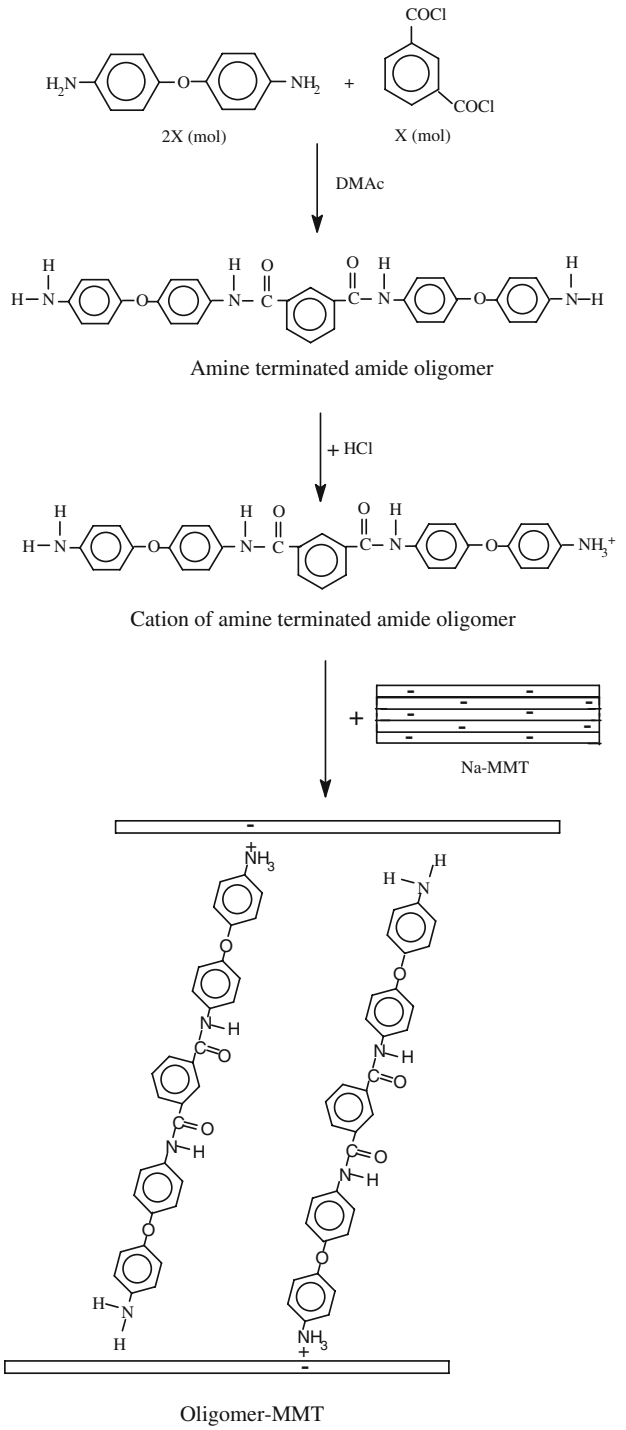

Scheme 1 Schematic representation for the formation of amine terminated amide oligomer and oligomer-MMT

precipitates of organoclay were collected by filtration and washed repeatedly with DMSO to remove the residual ammonium salt of oligomer until no AgCl precipitates identified with $AgNO_3$ solution. These precipitates were dried in a vacuum oven at 60 °C for 24 h. The dried cake was ground and screened with a 325-mesh sieve. The powder obtained was termed as oligomer-MMT and used for the preparation of nanocomposites.

Synthesis of Aromatic–Aliphatic Polyamide Matrix

Aromatic–aliphatic polyamide matrix was synthesized by condensing 0.05 mol of 4-aminophenylsulfone with 0.05 mol of sebacoyl chloride in DMAc at low temperature and under anhydrous conditions. The reaction mixture was cooled to 0 °C in order to avoid any side reactions because the reaction was highly exothermic. After 1 h, the reaction mixture was allowed to come to ambient temperature and stirring was continued for 24 h to ensure the accomplishment of the reaction. To the reaction contents, 1% of sebacoyl chloride was added in order to generate carbonyl chloride terminal ends. The polyamide formed was viscous and golden yellow in color. To this polyamide solution, stoichiometric amount of TEA was added to quench HCl produced during the reaction. Centrifugation was carried out to separate the precipitates from the pristine polyamide resin. The above synthesized polyamide resin serve as a stock solution for nanocomposite formation. Scheme 2 illustrates the formation of aromatic–aliphatic polyamide chains.

Synthesis of Nanocomposite Films

Appropriate amounts of polyamide solution were mixed with oligomer-MMT to yield various concentrations ranging from 2 to 20 wt% of nanocomposite films. The mixture was stirred vigorously for 24 h at 25 °C in order to achieve uniform dispersion of organoclay in the polyamide matrix. Nanocomposite films were prepared by pouring the solutions into petri dishes, followed by solvent evaporation at 70 °C for 12 h. The nanocomposite films were further dried in vacuum oven at 80 °C to a constant weight. Scheme 2 represents the formation of aromatic–aliphatic polyamide/oligomer-MMT nanocomposites.

Characterization

FT-IR data for amide oligomer and thin polyamide film were recorded using Excalibur series FT-IR spectrometer, Model No. FTSW 3000MX (BIO-RAD). Weight-average (M_w) and number-average (M_n) molecular weights of polyamide was determined using a GPC equipped with Waters 515 pump. Absolute *N*, *N*-dimethylformamide (DMF) was used as an eluent monitored through a UV detector (UV S3702 at 270 nm) with a flow rate of 1.0 mL/min at 60 °C. XRD analysis was performed by a Philips PW 1820 diffractometer which uses Cu Kα as a radiation source. SEM micrographs were taken on a LEO Gemini 1530 scanning electron microscope at an accelerating voltage of 5.80 kV. The samples were fractured in liquid

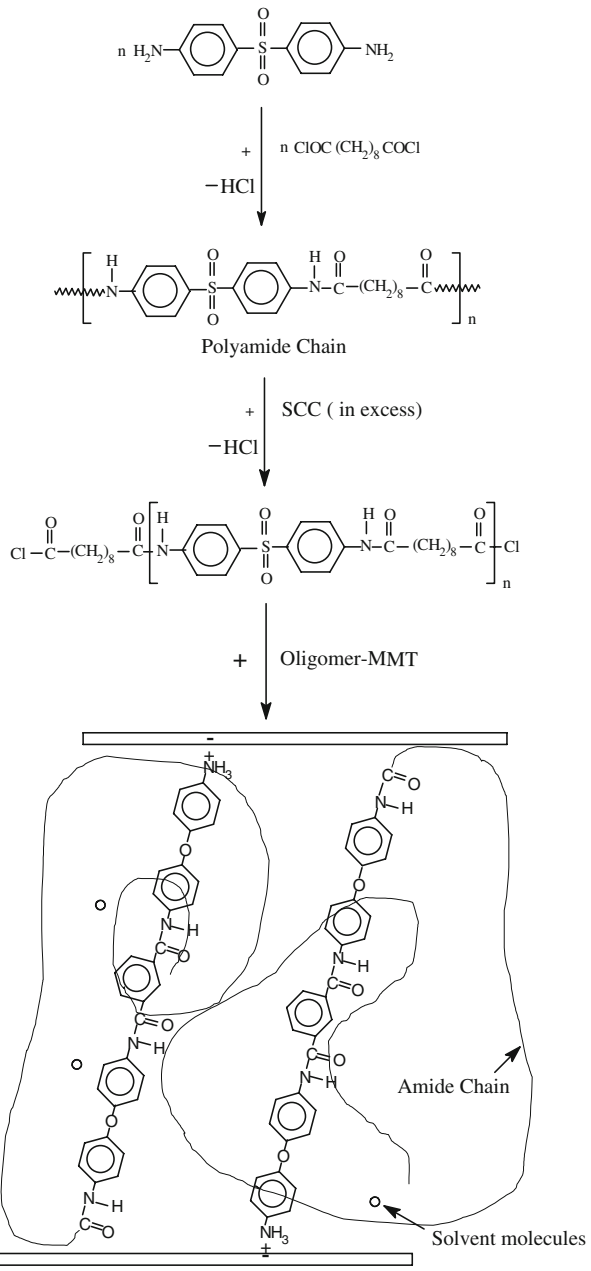

Scheme 2 Formation of carbonyl chloride end-capped aromatic–aliphatic polyamide chains and its nanocomposites with oligomer-MMT

nitrogen prior to imaging. TEM images were obtained at 200 kV with FEI Tecnai F20 transmission electron microscope. The nanocomposite films were first microtomed into 60 nm ultra thin sections with a diamond knife using Leica Ultracut UCT ultramicrotome. Tensile properties of the composite films (rectangular strips) were measured according to DIN procedure 53455 at 25 °C using Testometric Universal Testing Machine M350/500. Thermal stability of nanocomposites was determined using a METTLER TOLEDO TGA/SDTA 851[e] thermogravimetric analyzer at a heating rate of 10 °C/min under nitrogen. T_g of nanocomposites was recorded using a METTLER TOLEDO DSC 822[e] differential scanning calorimeter at a ramp rate of 10 °C/min in nitrogen atmosphere. The water uptake measurements of nanocomposites were performed under ASTM D570-81 procedure at 25 °C.

Results and Discussion

The chemical structure of amide oligomer was verified by infrared spectroscopy. The band appeared at 3262 cm^{-1} can be assigned to the N–H stretching vibration, while the band at 3035 cm^{-1} is due to the aromatic C–H stretching. Bands in the region of 1607 cm^{-1} to 1647 cm^{-1} are ascribed to the C=O groups in the oligomer. The group of closely related bands in the range of 1496 to 1525 cm^{-1} can be attributed to aromatic C=C stretching. A sharp band at 1215 cm^{-1} can be represented to the –C–O–C– stretching. Appearance of different IR bands in the spectrum confirmed the formation of amide oligomer. The pure polyamide film was transparent and golden in color. The same film was used for structure elucidation and molecular weight determination of the neat polyamide. Various IR bands appearing in the spectrum are 3324 cm^{-1} (N–H stretching), 3100 cm^{-1} (aromatic C–H stretching), 2930 cm^{-1} and 2857 cm^{-1} (CH_2 asymmetric and symmetric stretching), 1681 cm^{-1} (C=O group), 1588 cm^{-1} (aromatic C=C stretching), 1315 cm^{-1} and 1152 cm^{-1} (S=O asymmetric and symmetric stretching). The IR data confirms the formation of the aromatic-aliphatic polyamide. The values of M_n, M_w, and polydispersity of polyamide were found to be 10133.10 g/mol, 20865.10 g/mol, and 2.06, respectively. The hybrid films were transparent at low concentration of organoclay while semitransparent and opaque at higher proportions of clay contents. In order to prepare polymer clay nanocomposites, *d*-spacing must be large and sufficiently organophilic to permit the entry of the organic polymer. The organic modifier used to replace the inorganic ions of clay is an ammonium ion of thermally stable amine terminated oligomer. These cations of the oligomeric species developed ionic bonding with clay and the other amine end of the oligomer could interact with polyamide matrix, producing mechanically stronger and thermally stable nanocomposites. These composite materials were investigated using various techniques.

X-ray Diffraction

XRD was exploited to characterize the microstructure of Na-MMT, a layered silicate with an interlayer spacing

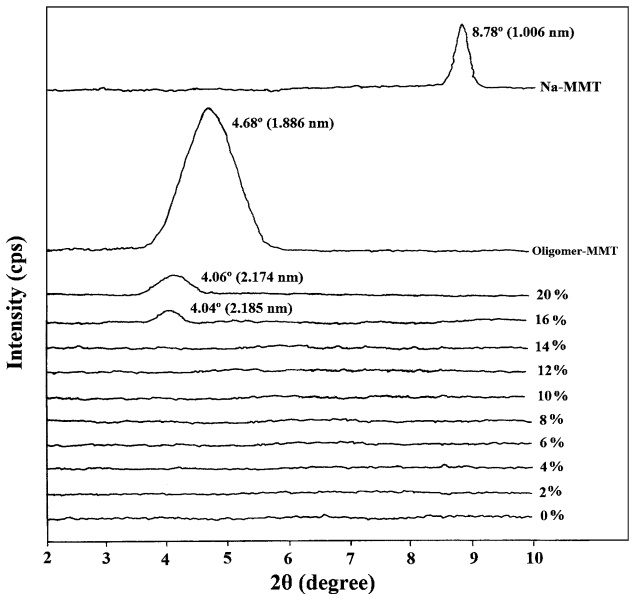

Fig. 1 X-ray diffraction curves of aromatic–aliphatic polyamide/oligomer-MMT nanocomposites

around 1.006 nm ($2\theta = 8.78°$). The organophilic MMT has a characteristic peak at low 2θ equal to 4.68° corresponding to a basal spacing of 1.886 nm. Data indicate that stiff and long chain structure of oligomer leads to the greater *d*-spacing of montmorillonite helping for the intercalation of polyamide into interlayers of clay. The XRD pattern for Na-MMT, neat polyamide, oligomer-MMT-based nanocomposites is shown in Fig. 1. Absence of diffraction peaks in XRD pattern of composites containing up to 14 wt% oligomer-MMT is indicative of the disruption of ordered platelets to a delaminated dispersion. An exfoliated dispersion was observed at low organoclay concentration. Increase in clay concentration from 16 to 20 wt% increases the basal spacing but the order is retained that appeared in the form of small peaks (Fig. 1) resulting in intercalated nanocomposites. At low clay concentration, polyamide clay interactions overcame the van der Waals forces between silicate interlayers resulting in complete disruption of clay structure. Due to an increase in clay concentration, van der Waals interactions dominated polymer clay interactions resulting in a finite expansion of silicate interlayers and retention of clay structure.

Scanning Electron Microscopy

SEM micrographs of fractured surface of the nanocomposites are presented in Fig. 2. These images did not exhibit inorganic domains at the maximum possible magnification, which means nanolayers are distributed well in the polyamide matrix. The absence of MMT particles indicates that the agglomerate is broken down to a size (submicron) that cannot be seen at this magnification. The thickness measured from the cross-sectional view of the micrograph (Fig. 2a) is found to be 0.28 mm.

Transmission Electron Microscopy

The state of delamination and intercalation inferred from XRD studies was further analyzed by TEM. Transmission electron micrographs of various polyamide-based oligomer-MMT nanocomposites are demonstrated in Fig. 3. Individual crystallites of the silicate are visible as regions of alternating narrow, dark, and light bands showing a strip distribution of silicate layers. Figure 3a shows a disruption of ordered platelet with an average platelet separation of 20 nm for polyamide/oligomer-MMT composites containing 6 wt% clay content. This is an indication of dominating delaminated dispersion. TEM photographs of 10 and 20 wt% nanocomposites are represented in Fig. 3b and c, respectively. These composites showed separation from 9 to 13 nm indicating an intercalated dispersion. The silicate dark lines have variable thickness due to stack of platelets one above each other and even high level of stacking occurred in the 20 wt% clay content. The trend in platelet spacing indicated by TEM matched with the XRD results.

Mechanical Properties

Tensile behavior of the system is shown in Table 1 and Fig. 4. The tensile strength of hybrid material increased up to 6 wt% oligomer-MMT (32.12 MPa) relative to the neat polyamide (18.86 MPa) and then decreased with further incorporation of organoclay. The tensile modulus increased up to 6 wt% oligomer-MMT, and then decreased with further addition of clay content. Both elongation at break point and toughness showed a decreasing behavior as compared to the pure polyamide. Mechanical data revealed improvements in the tensile strength of the hybrid materials because the stress is more efficiently transferred from the polymer matrix to the inorganic filler. Many polymeric matrices have been reinforced with MMT having no interphase interactions among the phases [47–49]. Polyimide-clay nanocomposites derived from poly(amic acid) and modified MMT with 12-aminododecanic and dodecylamine exhibited lower thermal expansion and gas permeation properties of composite films [8, 50]. These modifier developed no interaction with the poly(amic acid) and remained as low molecular weight compounds after imidization thus deteriorating the thermal and mechanical properties of resulting nanocomposites. However, when a modifier containing two amine functional groups were employed where one cationic end of modifier replaced with the negatively charged silicate layers while the other group of the swelling agent reacted with poly(amic acid)

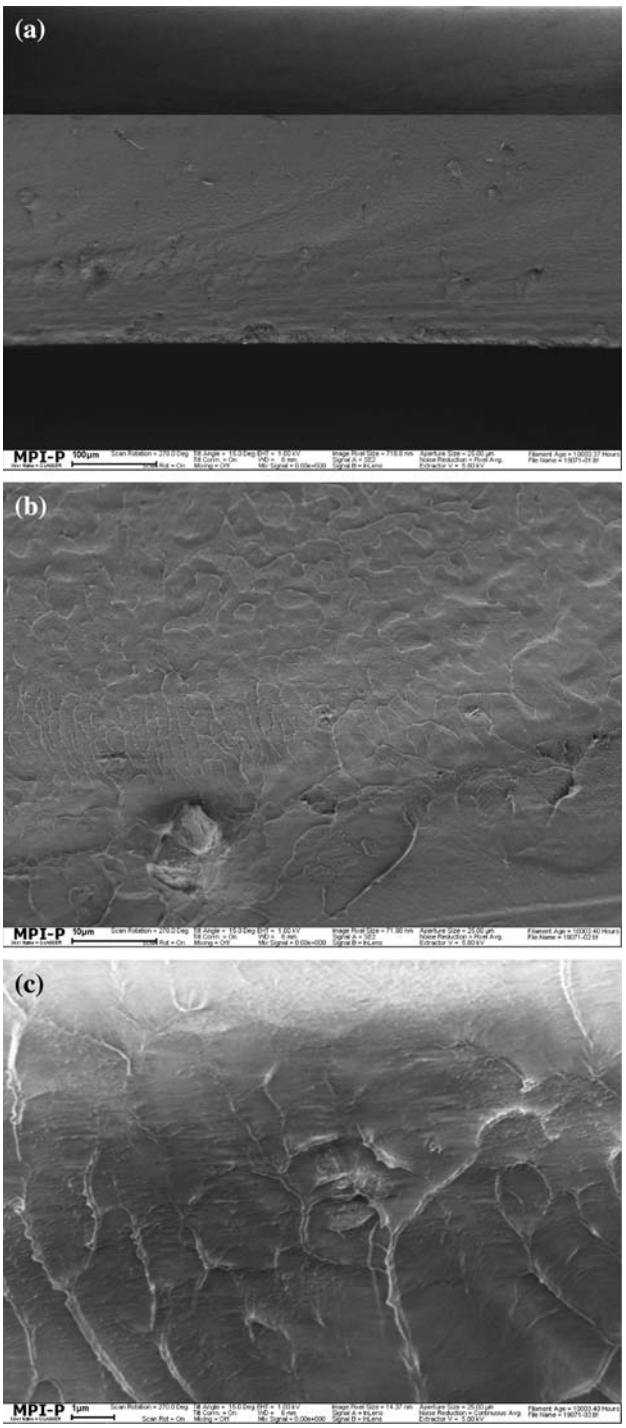

Fig. 2 SEM micrographs of aromatic–aliphatic polyamide-based nanocomposites containing 6 wt% oligomer-MMT

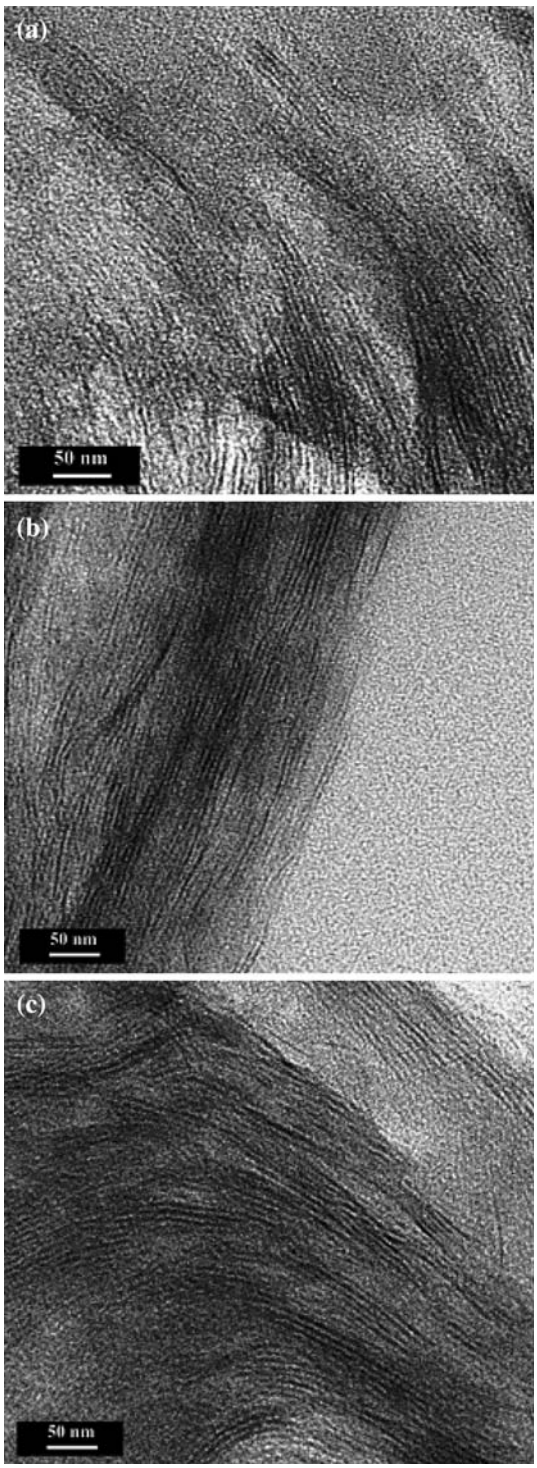

Fig. 3 TEM micrographs of aromatic–aliphatic polyamide-based nanocomposites containing **a** 6 wt%, **b** 10 wt%, **c** 20 wt% oligomer-MMT

molecules diffused into space between the nanolayers of MMT. In this way, modifier attached chemically to the organoclay yielding mechanically stronger nanocomposites. Similarly, chemically bonded and unbonded nanocomposites based on polyamides have also been documented by the present authors using both sol-gel and solution intercalation techniques [5–7, 23, 24, 26–28]. Enhancement in modulus results due to strong interactions through chemical and hydrogen bonding between the polyamide matrix and layered silicate. Nevertheless upon

high loading of oligomer-MMT, silicate layers may stack together in the form of crystallites and interlayer spaces do not expand much, limiting the diffusion of the polymer chains and deteriorating the mechanical properties.

Thermogravimetric Analysis

Thermal stability of the polyamide/oligomer-MMT composites determined under inert atmosphere is shown in Fig. 5. Thermal decomposition temperatures of the nanocomposites were found in the range 400–450 °C. However, the pure polyamide shows initial weight loss between 100 and 200 °C, which may be due to the removal of moisture and/or some volatiles. Thermograms indicated that nanocomposites are thermally stable, which increased with the addition of oligomer-MMT in the polyamide. Nanocomposites prepared from polyamides and different ceramic phases showed enhanced thermal stability upon the addition of these inorganic materials [23, 24, 27, 28]. The weight retained at 800 °C is roughly proportional to the amount of organoclay in the nanocomposites. Inclusion of the inorganic filler into the organic phase was found to increase the thermal stability presumably due to superior insulating features of the layered silicate which also acts as mass transport barrier to the volatile products generated during decomposition.

Differential Scanning Calorimetry

The glass transition temperatures of nanocomposites were recorded using DSC technique that increased with augmenting organoclay contents (Table 1). These results described a systematic increase in the T_g values as a function of organoclay showing greater interaction between the two disparate phases. The maximum T_g value (91.87 °C) was obtained with 16 wt% addition of

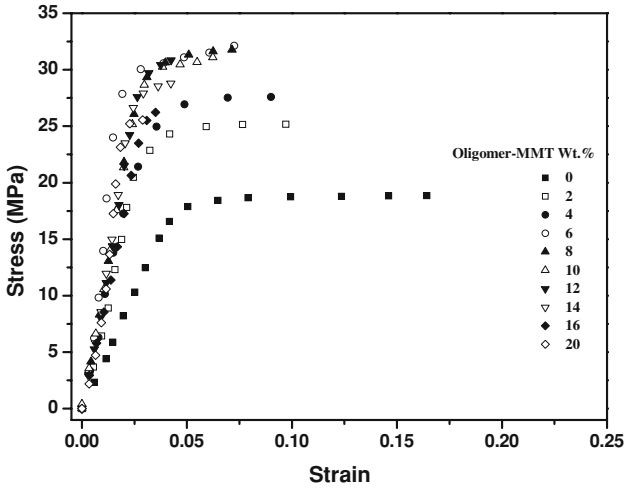

Fig. 4 Stress–strain curves of aromatic–aliphatic polyamide/oligomer-MMT nanocomposites

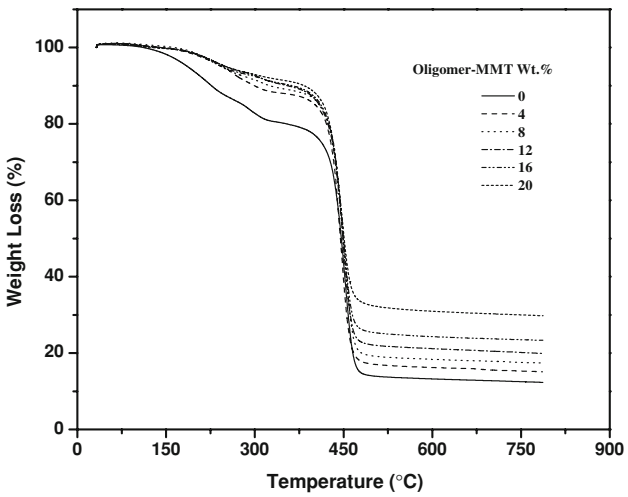

Fig. 5 TGA curves of aromatic–aliphatic polyamide/oligomer-MMT nanocomposites obtained at a heating rate of 10 °C min^{-1} in nitrogen

Table 1 Mechanical data of aromatic–aliphatic polyamide/oligomer-MMT hybrid materials

Oligomer-MMT contents (%)	Maximum stress (MPa) ± 0.10	Maximum strain ± 0.02	Initial modulus (MPa) ± 0.02	Toughness (MPa) ± 0.20	T_g (°C) ± 0.03	Water absorption at equilibrium (%)
0.0	18.86	0.164	386.64	2.629	72.34	16.1
2.0	25.18	0.097	686.36	2.006	–	15.5
4.0	27.58	0.090	803.02	1.986	74.57	14.8
6.0	32.12	0.073	1063.08	1.903	–	14.2
8.0	31.77	0.072	983.74	1.753	76.09	13.3
10.0	31.10	0.062	937.24	1.445	–	12.8
12.0	30.85	0.043	891.42	0.832	81.48	12.6
14.0	28.78	0.042	889.19	0.818	–	10.6
16.0	26.23	0.035	838.83	0.513	91.87	9.2
20.0	25.56	0.029	726.85	0.432	89.82	9.1

organoclay relative to pristine polyamide (72.34 °C). Further inclusion of the oligomer-MMT decreased the T_g because the entire clay may not interact with the polymer matrix resulting in poor interfacial interactions. Introduction of modified clay impeded the segmental motion of the polymer chains and increased amount of organoclay shifted the baseline of DSC curve toward higher temperature. This also suggested that polyamide chains developed interactions with organophilic silicate layers. As a result, the motions of polymer chains were restricted, thereby, increasing the T_g values of the composite materials. Glass transition temperatures of nanocomposites increased for all the compositions studied. The change of glass transition temperature of the polymer composites relative to pure polyamide is attributed to the interaction between the filler and matrix at interfacial zones.

Water Absorption Measurements

The presence of silicate layers may be expected to decrease the water uptake due to a more tortuous path for the diffusing molecules that must bypass impenetrable platelets. The improved barrier characteristics, chemical resistance, reduced solvent uptake, and flame retardance of clay–polymer nanocomposites take advantage from the hindered diffusion pathways through the nanocomposite. The water uptake of composite materials measured under the saturation conditions (168 h) are shown in Table 1. The results showed maximum water absorption for the neat polyamide film 16.1% due to exposure of amide and sulfonyl polar groups to the surface of polymer where water molecules developed secondary bond forces with these polar groups. The increase in weight of the hybrid films due to uptake of water gradually decreased as the organoclay content in nanocomposites increased. This decrease is apparently due to the mutual interaction between the organic and inorganic phases. This interaction resulted in lesser availability of amide and sulfonyl groups to interact with water.

Conclusions

Aromatic–aliphatic polyamide/montmorillonite nanocomposites were synthesized using reactive thermally stable organoclay. The functionality of the swelling agent was adjusted in such a way that one of the amine ends formed an ionic bond with negatively charged silicates and the other free amino group in the modifier is available for further reaction with carbonyl chloride end-capped polyamide. Hence, enhanced morphology of polyamide/organoclay nanocomposites due to chemical bonding between the modifier and the polymer molecules resulted in improved mechanical and thermal properties. These thermally stable composites also exhibit considerable increase in T_g values and reduction in the water absorption.

Acknowledgments The authors appreciate the financial support provided by the Higher Education Commission of Pakistan (HEC) through project research grant 20-23-ACAD (R) 03-410. Sonia Zulfiqar is grateful to HEC for awarding her fellowship under "International Research Support Initiative Program" (IRSIP) to pursue research work at Max Planck Institute for Polymer Research (MPI-P), Mainz, Germany. Special thanks are due to Prof. Dr. Gerhard Wegner, Director, MPI-P, for providing the characterization facilities for the completion of this work.

References

1. E.P. Giannelis, Adv. Mater. **8**, 29 (1996). doi:10.1002/adma.19960080104
2. Z. Wang, T.J. Pinnavaia, Chem. Mater. **10**, 1820 (1998). doi:10.1021/cm970784o
3. S.D. Burnside, E.P. Giannelis, Chem. Mater. **7**, 1597 (1995). doi:10.1021/cm00057a001
4. M. Alexandre, P. Dubois, Mater. Sci. Eng. **28**, 1 (2000). doi:10.1016/S0927-796X(00)00012-7
5. S. Zulfiqar, Z. Ahmad, M. Ishaq, S. Saeed, M.I. Sarwar, J. Mater. Sci. **42**, 93 (2007). doi:10.1007/s10853-006-1082-8
6. A. Kausar, S. Zulfiqar, S. Shabbir, M. Ishaq, M.I. Sarwar, Polym. Bull. **59**, 457 (2007). doi:10.1007/s00289-007-0786-5
7. N. Bibi, M.I. Sarwar, M. Ishaq, Z. Ahmad, Polym. Polym. Compos. **15**, 313 (2007)
8. Y. Yano, A. Usuki, T. Kurauchi, O. Kamigato, J. Polym. Sci. Part A Polym. Chem. **31**, 2493 (1993). doi:10.1002/pola.1993.080311009
9. P.B. Messersmith, E.P. Giannelis, Chem. Mater. **6**, 1719 (1994). doi:10.1021/cm00046a026
10. J.W. Gilman, Appl. Clay Sci. **15**, 31 (1999). doi:10.1016/S0169-1317(99)00019-8
11. J.W. Gilman, T. Kashiwagi, M. Nyden, J.E.T. Brown, C.L. Jackson, S. Lomakin, E.P. Giannelis, E. Manias, *Chemistry and Technology of Polymer Additives* (Royal Society of Chemistry, Cambridge, England, 1999), p. 249
12. J.W. Gilman, C.L. Jackson, A.B. Morgan, R. Harris Jr., E. Manias, E.P. Giannelis, M. Wuthenow, D. Hilton, S.H. Phillips, Chem. Mater. **12**, 1866 (2000). doi:10.1021/cm0001760
13. Z. Shen, G.P. Simon, Y.B. Cheng, Polymer (Guildf) **43**, 4251 (2002). doi:10.1016/S0032-3861(02)00230-6
14. A.B. Morgan, J.W. Gilman, J. Appl. Polym. Sci. **87**, 1329 (2003). doi:10.1002/app.11884
15. A. Okada, M. Kawasumi, A. Usuki, Y. Kojimi, T. Kurauchi, O. Kamigato, Mater. Res. Symp. Proc. **171**, 45 (1990)
16. A. Usuki, Y. Kojima, M. Kawasumi, A. Okada, Y. Fukushima, T. Kurauchi, O. Kamigaito, J. Mater. Res. **8**, 1179 (1993). doi:10.1557/JMR.1993.1179
17. B. Hoffmann, J. Kressler, G. Stopplemann, C. Friedrich, G.-M. Kim, Colloid Polym. Sci. **278**, 629 (2000). doi:10.1007/s003960000294
18. X. Liu, Q. Wu, Q. Zhang, L.A. Berglund, Z. Mo, Polym. Bull. **48**, 381 (2002). doi:10.1007/s00289-002-0051-x
19. N. Hasegawa, H. Okamoto, M. Kato, A. Usuki, N. Sato, Polymer (Guildf) **44**, 2933 (2003). doi:10.1016/S0032-3861(03)00215-5
20. R.K. Ayyer, A.I. Leonov, Rheol. Acta **43**, 283 (2004). doi:10.1007/s00397-003-0343-6
21. S. Zulfiqar, Z. Ahmad, M.I. Sarwar, Colloid Polym. Sci. **285**, 1749 (2007). doi:10.1007/s00396-007-1768-8

22. S. Zulfiqar, I. Lieberwirth, M.I. Sarwar, Chem. Phys. **344**, 202 (2008). doi:10.1016/j.chemphys.2008.01.002
23. M.I. Sarwar, S. Zulfiqar, Z. Ahmad, J. Sol-Gel Sci. Technol. **45**, 89 (2008). doi:10.1007/s10971-007-1640-9
24. M.I. Sarwar, S. Zulfiqar, Z. Ahmad, Colloid Polym. Sci. **285**, 1733 (2007). doi:10.1007/s00396-007-1760-3
25. S. Zulfiqar, M.I. Sarwar, High Perform. Polym. (2009). doi: 10.1177/0954008308089114
26. M.I. Sarwar, S. Zulfiqar, Z. Ahmad, Polym. Int. **57**, 292 (2008). doi:10.1002/pi.2343
27. M.I. Sarwar, S. Zulfiqar, Z. Ahmad, J. Sol-Gel Sci. Technol. **44**, 41 (2007). doi:10.1007/s10971-007-1591-1
28. M.I. Sarwar, S. Zulfiqar, Z. Ahmad, Polym. Compos. **30**, 95 (2009). doi:10.1002/pc.20538
29. Y.W. Park, J.E. Mark, Colloid Polym. Sci. **278**, 665 (2000). doi: 10.1007/s003960000316
30. P.W. Morgan, *Condensation Polymers by Interfacial and Solution Methods* (Interscience, New York, 1965)
31. W.B. Black, J. Preston, in *Man Made Fibers*, ed. by H. Mark, S.M. Atlas, E. Cernia (Interscience, New York, 1968), p. 306
32. F.G. Lum, E.F. Carlston, Ind. Eng. Chem. **44**, 1595 (1952)
33. F.G. Lum, E.F. Carlston, Ind. Eng. Chem. **49**, 1239 (1957)
34. R.G. Beaman, P.W. Morgan, C.R. Koller, E.L. Wittbecker, J. Polym. Sci. **40**, 329 (1959). doi:10.1002/pol.1959.1204013703
35. V.E. Shashoua, W.M. Eareckson, J. Polym. Sci. **40**, 343 (1959). doi:10.1002/pol.1959.1204013705
36. H. Hopff, A. Krieger, Makromol. Chem. **47**, 93 (1961). doi: 10.1002/macp.1961.020470109
37. B.S. Gorton, J. Appl. Polym. Sci. **9**, 3753 (1965). doi:10.1002/app.1965.070091122
38. W.H. Bonner, U.S. Patent 3,325,342, 1967, assigned to the Du Pont Co
39. A.C. Davis, T.E. Edwards, British Patent 1,070,416, 1967, assigned to Imperial Chemical Industries, Ltd
40. P.W. Morgan, S.L. Kwolek, J. Polym. Sci. **62**, 33 (1962). doi: 10.1002/pol.1962.1206217304
41. P.W. Morgan, S.L. Kwolek, Macromolecules **8**, 104 (1975). doi: 10.1021/ma60044a003
42. L. Shi, S. Gunasekaran, Nanoscale Res. Lett. **3**, 491 (2008). doi: 10.1007/s11671-008-9185-6
43. J.J. George, A.K. Bhowmick, Nanoscale Res. Lett. **3**, 508 (2008). doi:10.1007/s11671-008-9188-3
44. P.S. Kishore, B. Viswanathan, T.K. Varadarajan, Nanoscale Res. Lett. **3**, 14 (2008). doi:10.1007/s11671-007-9107-z
45. W. Yang, J. Liu, R. Zheng, Z. Liu, Y. Dai, G. Chen, S. Ringer, F. Braet, Nanoscale Res. Lett. **3**, 468 (2008). doi:10.1007/s11671-008-9182-9
46. P.K. Gutch, S. Banerjee, D.K. Jaiswal, J. Appl. Polym. Sci. **89**, 691 (2003). doi:10.1002/app.12157
47. H.L. Tyan, Y.C. Liu, K.H. Wei, Chem. Mater. **11**, 1942 (1999). doi:10.1021/cm990187x
48. H.L. Tyan, K.H. Wei, T.E. Hsieh, J. Polym. Sci. Part B Polym. Phys. **38**, 2873 (2000)
49. H.L. Tyan, C.M. Leu, K.H. Wei, Chem. Mater. **13**, 222 (2001). doi:10.1021/cm000560x
50. T. Lan, P.D. Kaviratna, T.J. Pinnavaia, Chem. Mater. **6**, 573 (1994). doi:10.1021/cm00041a002